Ultrasound Fourier Slice Imaging: a novel approach for ultrafast imaging technique

Olivier Bernard, *Member, IEEE,* Miaomiao Zhang, François Varray, *Member, IEEE,*
Jean-Philippe Thiran, *Member, IEEE,* Hervé Liebgott, *Member, IEEE,* and Denis Friboulet, *Member, IEEE*

***Abstract*—Ultrafast imaging based on plane-wave (PW) is an active area of research thanks to its capability of reaching frame rate higher than a thousand of frames per second. Several approaches that have been proposed are based on Fourier-domain reconstruction. In these techniques, the Fourier transform of the received echo is projected to the k-space corresponding to the Fourier transform of the object function. For one emitted PW, N lines along the kz axis direction are reconstructed in the k-space. We propose in this study a new acquisition scheme which allows acquiring the non-null part of the ultrasound spectrum with finer resolution. We shows that this strategy allows obtaining images with slightly better lateral resolution and higher contrast-to-noise ratio (CNR) when compared to other Fourier-based techniques.**

***Index Terms*—Plan wave, Fourier imaging, Ultra-fast imaging**

I. Introduction

Ultrafast ultrasound imaging faces an increasing interest in the ultrasound community due to its capacity to acquire high frame rate imaging with comparable image quality than the one obtained using conventional techniques. These methods are based on the insonification of a medium using one or several plane waves for compounding purposes. Assuming that the only limitation for the frame rate is the waves propagation time, the image frame rate of ultrasfast imaging system is no longer limited by the number of firing required to acquire a full image but by the time of a single pulse to propagate in the medium and get back to the transducer, which could attain very high frame rate (up to 5000 frames per second for a 15 cm depth scan using only one plane wave) and thus presents strong potential to improve tissue motion estimation and characterization.

The existing ultrasfast methods could be classified in two groups: spatial-based approaches where the images are directly computed from the space domain [1], [2] and Fourier-based techniques where the received raw-data is used to reconstruct the Fourier spectrum of the image of interest [3], [4]. In this study, we focus on the second group of methods. In these techniques, the following generic scheme is used. One plane wave is first emitted. Backscattered echos are then measured (Fig. 1-a). 2D-Fourier transform is applied on the received image and non-evanescence acoustic wave properties are then applied (Fig. 1-b). Finally, a remapping function is used to project the Fourier transform of the received echo to the k-space corresponding to the Fourier transform of the object function (Fig. 1-c). By taking the inverse 2D-Fourier transformed, the final ultrasound image is then reconstructed.

O. Bernard, M. Zhang, F. Varray, H. Liebgott and D. Friboulet are with the University of Lyon, CREATIS, CNRS UMR5220, Inserm U630, INSA-Lyon, University of Lyon 1, Villeurbanne, France (e-mail: firstname.lastname@creatis.insa-lyon.fr.

J.P. Thiran is with the Ecole Polytechnique fédérale de Lausanne (EPFL), Signal Processing Laboratory (LTS5), Switzerland.

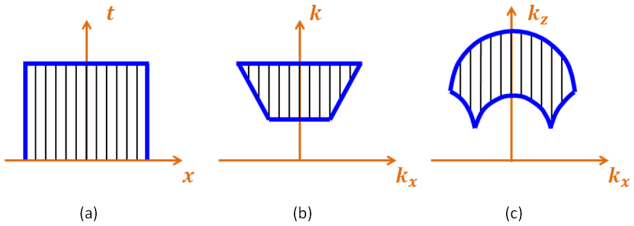

Fig. 1. Reconstruction procedure for conventional Fourier-based technique

One important shared property of the above mentioned Fourier-based techniques is that the Fourier spectrum of the object is sampled along the kz axis direction with a lateral step proportional to the inverse of the pitch (distance between two consecutive active elements) which limits the access to the central part of the spectrum. Keeping in mind the intrinsic demodulation nature of ultrasound images, we propose in this study a new Fourier-based acquisition scheme better suited to the spectral properties of such images. In particular, we propose an ultrasound Fourier slice imaging technique which allows sampling the Fourier spectrum of the object radially. By doing so, the useful information of the spectrum is more evenly sampled compared to the existing Fourier-based techniques.

The paper is organized as follows. In Section II, the new ultrasound acquisition scheme is described. In particular we show how Fourier slice imaging theory could be exploited to reconstruct ultrasound images. The quality of the obtained images is then investigated through both numerical simulation and experimental data in Section III. Comparisons with the two others Fourier-based techniques are also provided. Finally, concluding remarks are given in Section IV.

II. Methodology

A. Steered plane-wave

The concept of ultrasound Fourier slice imaging is based on the use of a steered plane-waves. Let $\phi_{\mathbf{n}}(\mathbf{x})$ be a plane-wave steered in the direction defined by $\mathbf{n}$. This plane-wave could be defined as:

$$\phi_{\mathbf{n}}(\mathbf{x},t) = \phi\left(ct - \mathbf{n}\cdot\mathbf{x}\right) \tag{1}$$

The ultrasound steered plane-wave could thus be rewritten as:

$$\phi_{\mathbf{n}}(\mathbf{x},t) = \phi(ct) * \delta\left(ct - \mathbf{n}\cdot\mathbf{x}\right) = \phi * \delta\left(ct - \mathbf{n}\cdot\mathbf{x}\right) \quad (2)$$

The wave front of a propagating field corresponds to the place, at a particular time instant t_0, where the field value is the same, *i.e.* $\{\mathbf{x}\}$ verifying $\phi(\mathbf{x}, t_0) = cst$. In the particular case of steered plane-wave, thanks to equation (2), the corresponding wave front could be easily defined as the place where $\delta\left(ct_0 - \mathbf{n}\cdot\mathbf{x}\right) = 0$, *i.e.* $\mathbf{n}\cdot\mathbf{x} = ct_0$ which corresponds to a line perpendicular to the direction given by $\mathbf{n}$ and passing through the point $ct_0\,\mathbf{n}$.

B. Ultrasound image formation

The ultrasound image formation process we propose is based on the used of steered plane-waves both in emission and reception as illustrated in Fig. (2).

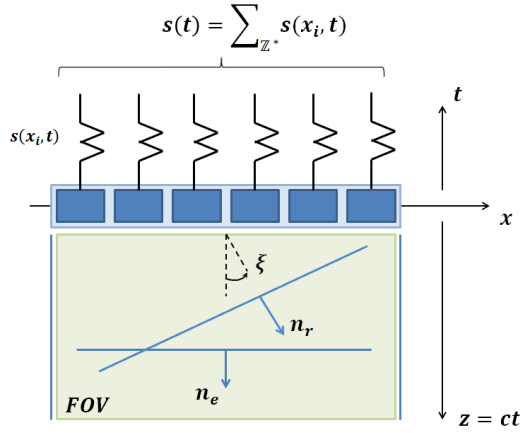

Fig. 2. Illustration of image formation using Ultrasound Fourier Slice Imaging scheme

The output signal of such a system could be modelized as follows [3]:

$$\begin{aligned} s(t) &= \sum_{\mathbb{Z}^*} s(x_i,t) \quad (3)\\ &= \iint_{FOV} m(\mathbf{x})\cdot\phi_{\mathbf{n}_e}(\mathbf{x}) * \phi_{\mathbf{n}_r}(\mathbf{x})\,\mathrm{d}\mathbf{x}\\ &= \iint_{FOV} m(\mathbf{x})\cdot\phi_{er} * \delta\left(ct - \mathbf{n}_{er}\cdot\mathbf{x}\right)\,\mathrm{d}\mathbf{x}, \end{aligned}$$

where $\mathbb{Z}^*$ corresponds to the restriction of $\mathbb{Z}$ to the probe dimensions. $m(\cdot)$ is a function that characterizes both the spatial distribution and the backscattered amplitude of the different scatterers present in the insonified medium $M \in \mathbb{R}^2$. Typically, $m(\cdot)$ could be defined as:

$$m(\mathbf{x}) = \sum_{\{i,j,k\}\in FOV} a(i,j,k)\delta(x-i)\cdot\delta(y-j)\cdot\delta(z-k) \quad (4)$$

C. Ultrasound Fourier Slice Imaging concept

The temporal Fourier transform of signal $s(t)$ leads to the following relation:

$$\mathcal{F}_t\left(s(t)\right) = \int_{\mathbb{R}} \left[\iint_{FOV} m(\mathbf{x})\cdot\phi_{er} * \delta\left(ct - \mathbf{n}_{er}\cdot\mathbf{x}\right)\,\mathrm{d}\mathbf{x}\right] \mathrm{e}^{-j2\pi ft}\,\mathrm{d}t. \quad (5)$$

Given the fundamental relations $z = ct$ and $k = \frac{2\pi f}{c}$, where z and k corresponds to the spatial distance and the wavenumber defined in the direction given by $\mathbf{n}_{er}$, respectively, equation (5) can be rewritten as:

$$\mathcal{F}_t\left(s(t)\right) = \frac{1}{c}\int_{\mathbb{R}} \left[\iint_{FOV} m(\mathbf{x})\cdot\phi_{er} * \delta\left(z - \mathbf{n}_{er}\cdot\mathbf{x}\right)\,\mathrm{d}\mathbf{x}\right] \mathrm{e}^{-jkz}\,\mathrm{d}z. \quad (6)$$

Using Fourier slice theorem, equation (6) could be interpreted as the $2D$-spatial Fourier transform of the image $(m\ \cdot\ \phi_{er})(\cdot)$ restricted to the line of direction $\mathbf{n}_{er}$. In the special case where $\mathbf{n}_e = (0,1)^T$ and $\mathbf{n}_r = (\sin(\xi_i), \cos(\xi_i))^T$, the following relations could be derived:

$$\begin{cases} k_x = k\,n_{xr} = k\,\sin(\xi_i) \\ k_z = k\,(n_{ze} + n_{zr}) = k\,(1+\cos(\xi_i)) \end{cases} \quad (7)$$

and

$$\begin{cases} k = \frac{k_x^2 + k_z^2}{2\,k_z} \\ \xi_i = \arctan\left(\frac{k_x}{k_z - k}\right) = \arctan\left(\frac{2\,k_x\,k_z}{k_z^2 - k_x^2}\right) \end{cases} \quad (8)$$

As a consequence, when the emitted field is a plane-wave perpendicular to the probe and the received field is supposed to be a steered plane-wave with angle ξ_i, equations (6)-(8) show that the temporal Fourier transform of the received signal is equal to a radial line of angle $\theta_i = f(\xi_i)$ (with $f(\cdot) = atan(sin(\cdot)/(1+cos(\cdot)))$) in the corresponding k-space domain. By simply playing with different delay strategies applied on the received signals, we are thus able, for only one emitted plane-wave, to radially and densely recover the Fourier space of the object and thus reconstruct an ultrasound image with high frame rate.

D. Spectral acquisition scan

1) Bandwidth of the transducer: Because of the limited bandwidth of sensors and excitation pulse, the spectrum can only be measured in the spatial bandwidth corresponding to the bandwidth of the excitation signal $k_{min} < k < k_{max}$. The k range is larger if broadband excitation impulse and broadband transducer are used.

2) Steered angle in reception: Because of the limited size D of the ultrasound phased array, ξ_i is constrained in the interval $-\xi_{max} < \xi_i < \xi_{max}$. ξ_{max} can be expressed by:

$$\xi_{max} = \arctan\left(\frac{D}{2\,z_{max}}\right) \quad (9)$$

This expression can be deduced from geometrical considerations. If ξ_i is too high, the deep medium is not insonified and the image can't be reconstructed. The above relation guaranties that at least half of medium is insonified at z_{max}.

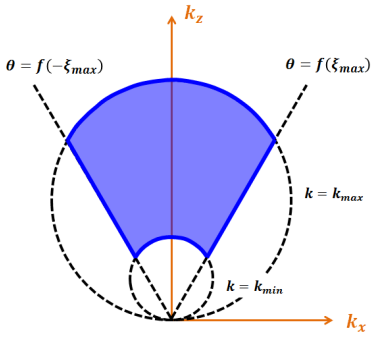

Fig. 3. Fourier plan of the ultrasound image - The area striped with vertical lines (respectively horizontal) corresponds to the area where the condition on ξ is verified (respectively the condition on k is verified).

3) Reachable image spectrum: When fixing ξ_i in equation (7), one can show that the corresponding curve in the image spectrum is a line passing by the origin with angle $\theta_i = f(\xi_i)$. Therefore the accessible range of ξ_i corresponds to a cone of apex ξ_{max}. When fixing k in (7), one can show that the corresponding curve in the image spectrum is a circle centered at $(k_x, k_z) = (0, k)$, with a diameter of $2k$. Since the two conditions must be verified simultaneously, the accessible area is the intersection between the steering angle and frequency limitation area, as shown in Fig. 3. The acquisition scheme corresponding to the proposed approach is summarized through Fig. 4.

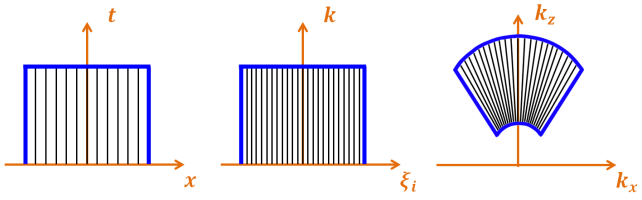

Fig. 4. Reconstruction procedure with the proposed method

III. Results

The performance of the proposed method has been evaluated from both simulation and experimental data. The CREANUIS software [5] was used to simulate ultrasound raw-data beamformed with either classical delay and sum (DAS) method or using a plane wave as required by the Fourier-based techniques. For the experimental data, we used a UlaOp ultrasound scanner [6]. The involved probe is a 1-D linear array whose properties are given in Table I. The same probe settings were used for both simulations and experiments with the exception of the number of active elements in the simulation in order to acquire a wider tissue region (83 elements for a 2mm width phantom). In the case of classical imaging (DAS), the transmit focus value was set to half the maximum depth of the phantom.

A. Spatial resolution

The image quality of the proposed method has first been investigated experimentally through the measurement of spatial resolution using the UlaOp system. The physical phantom involved in this experiment corresponds to a 300μm nylon wire in a water tank and positioned at different depths from the probe (15mm to 35mm each 5mm). For comparison purposes, we recorded for each experiment the B-mode image delivered by the equipment (obtained from a conventional DAS technique) and the raw-data generated by the emission of a single plane wave to reconstruct images using Lu, Garcia and our proposed approach.

TABLE I
Probe settings

Parameters	Value
Transmit frequency	5 MHz
Sampling frequency	50 MHz
Number of active elements	64
Pitch	264 μm
Kerf	44 μm
Height	5 mm
Apodization	None
Transmit focus	Depends on acquisition mode

Table II shows the measured axial and lateral resolution as a function of the depth. It can be observed that the measured axial resolution is almost the same and closed to 1mm for all the methods, which is in the order of the excitation pulse length (set as 3 cycles of the excited signal having a wavelength of 0.3mm). It is also interesting to note that the proposed method yields better lateral resolution compared to the two others Fourier-based techniques, whatever the depth. Indeed, the measured lateral resolution is in the range $[1.84-1.98]$mm using the proposed method, $[2.47-3.11]$mm with Lu's method, and $[1.91-2.99]$mm with Garcia's method. When compared to the DAS technique, the lateral resolution corresponding to our approach is slightly higher, with a difference of 0.34mm in average.

In order to illustrate the obtained results, we display in Fig. 5 the different images obtained when the phantom is placed at 30mm of depth from the probe. In this example, the measured PSF was [0.95 x 1.27]mm with the DAS method, [1.00 x 1.86]mm with the proposed approach, [1.05 x 3.11]mm with Lu's method and [0.97 x 2.99]mm with Garcia's method.

B. Contrat-to-noise ratio

The quality of the reconstructed image was then further investigated from contrast-to-noise ratio (CNR) measurements performed through numerical simulations. The simulated phantoms are composed of 100.000 scatterers uniformly

TABLE II
Spatial resolution values measured from the UlaOp ultrasound scanner

Spatial resolution (mm)		DAS		Proposed meth.		Lu *et al.*		Garcia *et al.*	
		Axial	Lateral	Axial	Lateral	Axial	Lateral	Axial	Lateral
Depth (mm)	15	1,01	1,45	0,89	1,84	0,91	2,47	0,86	1,91
	20	1,02	1,62	0,86	1,84	0,86	2,72	0,88	2,33
	25	0,99	1,30	0,98	1,89	1,00	2,87	1,00	2,67
	30	0,95	1,27	1,00	1,86	1,05	3,11	0,97	2,99
	35	0,86	2,08	0,82	1,98	0,82	2,94	0,81	2,84

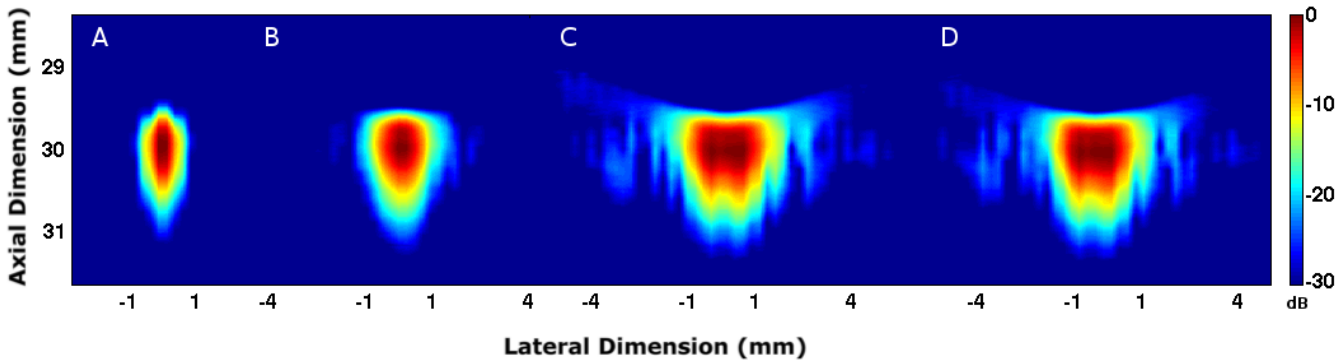

Fig. 5. PSF obtained from the UlaOp system using conventional delay-and-sum technique (A) and Fourier-based approaches: proposed method (B), Lu's method (C) and Garcia's method (D).

distributed in a region of dimensions 20mm x 20mm and at different depths (from 20mm to 60mm each 10mm).

Table III shows the measured CNR as a function of the depth. As for the previous experiments, the DAS approach gives the best scores, whatever the depth. This results is easily explained by the fact that this approach uses 64 times more firings than the Fourier-based methods, yielding to a higher amount of energy used to reconstruct one image. In terms of Fourier-based techniques, the proposed approach yields the best results, whatever the depth. In each case, the CNR improvement is in the order of 1dB.

TABLE III
CNR VALUES OBTAINED FROM SIMULATIONS USING CREANUIS SOFTWARE

CNR		DAS *mean ± std*	Proposed meth. *mean ± std*	Lu *et al.* *mean ± std*	Garcia *et al.* *mean ± std*
Depth (mm)	20	9,28 ± 0,30	6,44 ± 0,18	6,23 ± 0,34	4,35 ± 0,39
	30	10,31 ± 0,46	8,68 ± 0,33	7,69 ± 0,41	6,95 ± 0,41
	40	10,77 ± 0,27	8,56 ± 0,29	7,39 ± 0,42	7,1 ± 0,44
	50	10,71 ± 0,28	8,31 ± 0,19	6,89 ± 0,25	6,73 ± 0,28
	60	10,27 ± 0,22	7,71 ± 0,25	6,43 ± 0,24	6,34 ± 0,22

C. Fourier spectrum differences

Finally, the influence of the proposed acquisition scheme on the reconstructed spectrum is investigated. Fig. 6 shows the absolute difference of the Fourier spectra of a given simulated image obtained using the three different Fourier techniques. It can be observed that the difference of spectra between Lu and Garcia methods is null for the central part of the spectrum, yielding to comparable reconstructed ultrasound images. On the contrary, the difference in spectra between Lu and the proposed method is more dense with non-zero values all other the Fourier space. This illustrates the finer resolution we obtain with our approach, yielding to improvements in the quality of the reconstructed images.

IV. Conclusion

In this paper, we propose a new ultrasound acquisition scheme based on Fourier slice imaging. This technique allows acquiring the non-null part of the ultrasound spectrum with finer resolution thanks to a dedicated scheme. The quality and improvement of the reconstructed images were investigated through the measurements of spatial resolution and CNR values from numerical simulations and experimental data. In each case, the proposed method yields better results when compared to the others Fourier-based method.

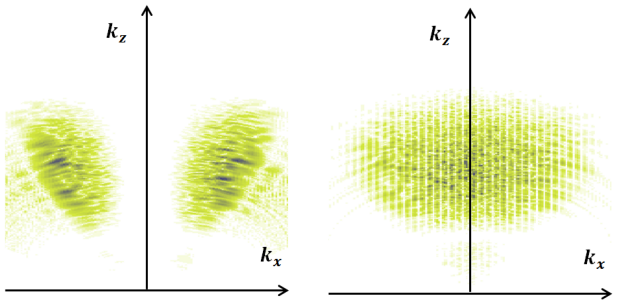

(a) Lu / Garcia diff. (b) Lu / proposed method diff.

Fig. 6. Spectrum mapping obtained from a simulated phantom. (a) Absolute differences of Lu's and Garcia's spectra. (b) Absolute differences of Lu's spectrum and the one obtained using the proposed framework.

References

[1] G. Montaldo, M. Tanter, J. Bercoff, N. Benech, and M. Fink, "Coherent plane-wave compounding for very high frame rate ultrasonography and transient elastography," *IEEE Transactions on Ultrasonics, Ferroelectrics and Frequency Control*, vol. 56, pp. 489–506, March 2009.

[2] C. Papadacci, M. Pernot, M. Couade, M. Fink, and M. Tanter, "High-contrast ultrafast imaging of the heart," *IEEE Transactions on Ultrasonics, Ferroelectrics and Frequency Control*, vol. 61, pp. 288–301, Feb 2014.

[3] J.-y. Lu, "2d and 3d high frame rate imaging with limited diffraction beams," *IEEE Transactions on Ultrasonics, Ferroelectrics and Frequency Control*, vol. 44, pp. 839–856, July 1997.

[4] D. Garcia, L. Tarnec, S. Muth, E. Montagnon, J. Porée, and G. Cloutier, "Stolt's f-k migration for plane wave ultrasound imaging," *IEEE Transactions on Ultrasonics, Ferroelectrics and Frequency Control*, vol. 60, pp. 1853–1867, Sep 2013.

[5] F. Varray, A. Ramalli, C. Cachard, P. Tortoli, and O. Basset, "Fundamental and second-harmonic ultrasound field computation of inhomogeneous nonlinear medium with a generalized angular spectrum method," *IEEE Transactions on Ultrasonics, Ferroelectrics and Frequency Control*, vol. 58, no. 7, pp. 1366–1376, 2011.

[6] P. Tortoli, L. Bassi, E. Boni, A. Dallai, F. Guidi, and S. Ricci, "Ulaop: an advanced open platform for ultrasound research," *IEEE Transactions on Ultrasonics, Ferroelectrics and Frequency Control*, vol. 56, no. 10, p. 2207–2216, 2009.